

XCXO: An Ultra-low Cost Ultra-high Accuracy Clock System for Wireless Sensor Networks in Harsh Remote Outdoor Environments *

Thomas Schmid, Jonathan Friedman, Zainul Charbiwala,
Young H. Cho, Mani B. Srivastava
Department of Electrical Engineering; University of California, Los Angeles
{schmid, jf, zainul, young, mbs}@ee.ucla.edu

1. INTRODUCTION

As the world ecosystem comes under increasing duress from the effects of global warming, volatile organic compounds (and other air pollutants), oil spills, pesticides, stronger coastal storms, and more frequent tornadoes and forest fires, early warning of and effective response to micro, local, and regional ecological problems is critical. Capturing this data is an immense challenge requiring long-term study over very large areas. Further, such a system must operate virtually free of infrastructure (power and hardline communications networks) to reduce the cost and environmental impact of deploying and maintaining it. Such systems, as envisioned by the scientific community, consist of a large quantity of sensors each attached to a small battery operated micro-processor replete with a radio communications transceiver. Each of these sensor terminals is called a node and the entirety of nodes is termed a Wireless Sensor Network (WSN). WSN's are, therefore, emerging as a vital element in humanity's response to a changing climate.

The single biggest impediment to a node's battery-powered lifetime is the energy spent during radio communication, and secondary to that, the time spent in its "awake" (as opposed to its low-power shutdown "sleep" state). Reduce these times, and lifetime improves substantially. However, as soon as nodes in the network begin sleeping and are correspondingly offline, other nodes in the network that are still awake can no longer use them as a communications hub to route sensor data back to a command-and-control station (referred to as a "gateway" node). To optimize sleep time and network performance simultaneously all of the nodes must synchronize their internal clocks and sleep and wake at the same time (we are aware that this statement is somewhat of a generality and numerous works on WSN scheduling exist, but our axiom to follow – that better synchrony yields better lifetime – still holds in these cases).

Commodity time references in WSN's, and indeed consumer and industrial products in general, typically consist of a quartz crystal driven by a Colpitts oscillator. This configuration is popular because it offers substantially better performance than switched resistive-capacitive networks

and ceramic-based mechanical resonators at a moderate and tolerable marginal cost (see Figure 1). However, crystals drift in frequency as their temperature changes. A survey of available HC-49S packaged crystals reveals that the majority of inexpensive parts experience a drift over the commercial temperature range (-20°C , $+70^{\circ}\text{C}$) of $\pm 50\text{ppm}$. With this much deviation, nodes must spend at least 0.01% of their lifetimes awake [16] in-order to guarantee that when they transmit, their intended receiver (whose clock has drifted differently) is awake to receive the broadcast. While this may sound acceptable, consider that a node that wants to sample water quality once per hour may only require a total of 100ms to wake, take the measurement, communicate any findings, and return to sleep. This corresponds to spending as little as 0.0028% of its lifetime awake. Repairing the temperature-imposed drift in the crystal-based clocks could improve network lifetime more than 3.5 times!

We propose a novel clock system (hardware and software) that is composed of two crystal oscillators running in parallel at each node. We then exploit the subtle manufacturing differences in each crystal that produce different drift-vs.-frequency behaviors. By measuring this difference we can compensate for the drifting clock. In effect, we have used one crystal to compensate the other, our concept, which we call XCXO (Crystal Compensated Crystal Oscillator). To verify, we fed temperature sensor data traces from a 3 year study of the James Wildlife Reserve in Riverside County, California, into Agilent 33220A Programmable Arbitrary Waveform Generators to recreate the oscillator under thermal conditions. In applying our XCXO architecture we observed an effective drift of only 0.04ppm or about *1 sec per year* – better performance than any commercial alternative available in its price/power class by at least a factor of 8.

2. CLOCK SOURCE CHARACTERISTICS

Timestamping of an event or network clock synchronization is usually performed by reading a hardware counter that is periodically updated by some system clock. The system clock runs at a rate of, say, $f\text{ Hz}$, incrementing the counter every $1/f\text{ sec}$. Therefore, at any time t since the n -bit counter was reset, it would read a count $c(t) = \lfloor f \cdot t \rfloor \bmod 2^n$. The floor operator $\lfloor \cdot \rfloor$ comes into play due to the digital nature of the hardware counter, which limits the precision with which one can measure time to $1/f\text{ sec}$. Most importantly, the accuracy with which we can measure time depends on how accurately we know the rate f at which the counter is incremented. Unfortunately, all clock implementations have some deviation from the nominal clock fre-

*This material is supported in part by the U.S. ARL and the U.K. MOD under Agreement Number W911NF-06-3-0001, by the NSF under award CNS-0614853, and by the Center for Embedded Networked Sensing at UCLA. Any opinions, findings and conclusions or recommendations expressed in this material are those of the authors and do not necessarily reflect the views of the listed funding agencies. The U.S. and U.K. Governments are authorized to reproduce and distribute reprints for Government purposes notwithstanding any copyright notation herein.

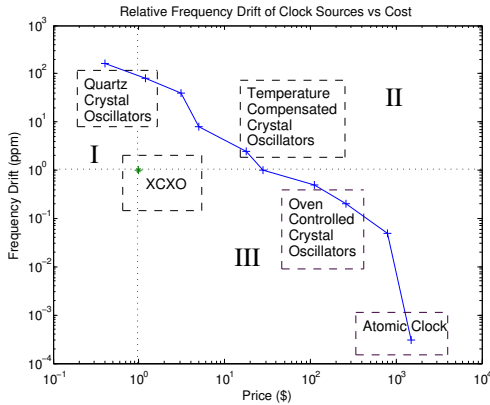


Figure 1: Relative Frequency Drift vs Cost of commercially available clock sources compared to our XCXO.

quency F_0 Hz that they are designed with.

The normalized deviation in frequency of a clock source from its nominal is termed its relative frequency drift or just *drift*¹, denoted as δf , and is measured in a unitless quantity called *ppm* or Parts Per Million. For a perspective on the values of drift, a consider a 10ppm clock source would introduce a measurement error of over 5 min per year. A 0.1ppm clock source on the other hand would be off by only about 3 sec over a year.

The three major factors affecting drift are manufacturing imprecision, temperature and aging. Other factors [2] include effects of humidity and pressure, acceleration effects (shock and gravity), effects due to electric and magnetic fields and particle radiation. In this design paper we focus only on effects due to the first two. The effects of humidity and pressure are effectively reduced by hermetically sealing the quartz crystal in the oscillator package.

The frequency drift of a quartz crystal based oscillator (due to the two factors) could be modeled as:

$$\delta f = \delta f_{tolerance} + \delta f_{stability}(T) \quad (1)$$

where $\delta f_{tolerance}$ is a constant drift in the range of 20-50ppm due to imprecision in the geometric cut of the crystal in the manufacturing process. $\delta f_{stability}$ is a non-linear temperature dependent factor that is usually in the range of 10-20ppm. Manufacturers of quartz crystal resonators and oscillators specify ranges for these values in datasheets as frequency tolerance and frequency stability respectively.

To produce a quartz resonator, manufacturers cut out a tiny sheet from a quartz crystal at a specific shear angle. Different angles of cut produce vastly different crystal characteristics. The most popular type is called AT-cut, which is cut at a nominal angle of $35^\circ 20'$, and accounts for up to 75% of all quartz resonators made due to its excellent frequency-temperature ($f - T$) characteristics. The $f - T$ characteristics of AT-cut crystals is well studied in the literature and is found to follow a third order polynomial using:

$$\delta f_{stability}(T) = A(T - T_0)^3 + B(T - T_0) + C \quad (2)$$

where A, B, C, T_0 are unique to each device. Interestingly, and this is the key observation behind the compensation

¹ Some researchers refer to this quantity as skew. Our definition follows the IEEE recommended standards [1].

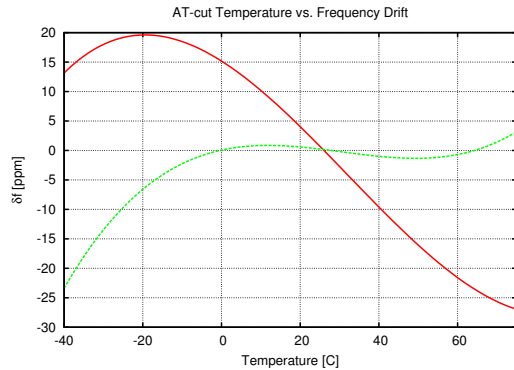


Figure 2: Frequency Drift vs Temperature for multiple AT-cut crystals. The crystals are cut at an angle of $35^\circ 20' + \theta$

techniques detailed later, the value of B is extremely sensitive to any imprecision in the angle of the cut itself. Figure 2 shows how the $f - T$ characteristics vary for AT-cut crystals sheared with a slightly different angle of cut. This slight difference could be either deliberate or due to manufacturing variation. The key idea behind improving the stability of the clock source is to exploit this difference in $f - T$ characteristics for two sources to compensate one of them.

Before we describe our XCXO compensation technique, it is noteworthy to mention the state-of-the-art in oscillator design. For mid-performance applications, designers prefer to use a temperature compensated crystal oscillator or TCXO [3–5]. The approach followed by a TCXO manufacturer is to characterize each device in the factory to obtain its $f - T$ curve [6]. Then, by using a custom analog matching circuit [7] or a digital tuning circuit with a temperature sensor [8–10], the $f - T$ characteristics are corrected by minuscule frequency adjustments to negate the effects of drift. For high-performance applications, designers employ an oven controlled crystal oscillator or OCXO which has an active mechanism maintaining the temperature of the crystal structure, allowing much higher frequency stability over external temperature variations at the cost of an active heating element.

Figure 1 shows how the stability of a clock source is related to its price. The x -axis could represent other cost parameters as well, such as power consumption and/or size without appreciable change. The three regions represent the spaces of crystals that (II) are cheaper, but less precise, (III) more expensive and less precise, and (I) better, but more expensive and power hungry than our XCXO solution.

2.1 Introducing Differential Drift

In order to explain how our XCXO compensation technique works, we first describe the mechanism intuitively. Assume that the system under consideration has two AT-cut quartz crystal oscillators with slightly different shearing angles. For now, we pick the crystals with the top and bottom curves from Figure 2 representing the $35^\circ 21'$ cut and the $35^\circ 28'$ cut. We first measure the 'difference of drift' between the two oscillators (or differential drift) over the entire temperature range and plot it against temperature, to obtain Figure 3. The reason that Figure 3 is almost a straight line is due to the fact that between the two crystals, it is the B parameter from Equation 2 that dominates. Now, if instead we plot the frequency drift of one of the oscillators

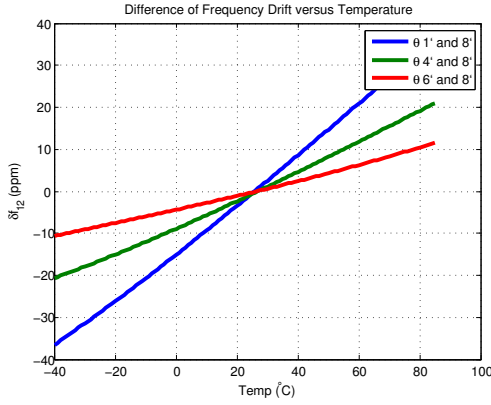


Figure 3: Differential Frequency Drift vs Temperature for multiple pairs of differently AT-cut oscillators. Note that the steeper the slope, the better it is for our compensation algorithm.

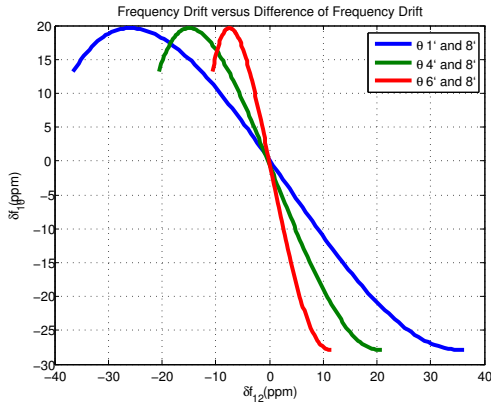


Figure 4: Frequency Drift versus Difference of Frequency Drift for several pairs of AT-cut oscillators. The larger the full span of δf_{12} the better our algorithm can compensate.

against the differential drift, we obtain Figure 4, which is similar to the $f - T$ curve of that oscillator. This leads us to believe that if the system measures the differential drift at run time, it can estimate the relative drift of one of its oscillators. Using this information, the system can make a correction to its oscillator when it deviates and thus gain higher frequency stability.

This approach is analogous to traditional temperature compensation techniques except that there are two significant advantages to compensating using differential drift. On the one hand, temperature sensing is itself error-prone, requiring its own calibration and compensation system to provide an appreciable accuracy in the reading. Further, temperature sensing displays non-linear dynamic behavior causing hysteresis effects during temperature variations. On the other hand, the measurement of differential drift is completely done in digital logic or software, and the accuracy of measurement can be set arbitrarily high. There are no dynamic behaviors that affect the reading and the speed of acquiring a reading scales with the speeds of deep sub-micron process technology. Additionally, the potential saving in hardware and thus production cost is tremendous since the logic circuitry could be directly integrated into microprocessors or systems on a chip (SoC) at virtually no additional

cost. To put it briefly, simpler hardware with smarter algorithms can yield lower production cost and performance advantages, as we will show.

3. CRYSTAL COMPENSATED CRYSTAL OSCILLATOR (XCXO)

The frequency correction algorithm is executed in two parts, a one time calibration phase and a run time compensation phase. The simplest implementation of the algorithm requires the software to have low level access to a hardware timer and two hardware counters. The authors believe it is feasible to relax this requirement to one counter in future implementations.

3.1 Calibration Phase

The calibration phase requires the use of two free running hardware counters C_1 and C_2 that are being fed from the two oscillators with frequencies f_1 and f_2 respectively. The system then captures the values of both counters at the positive edge of F_s , the reference clock, via an interrupt service routine and resets them to zero for the next sample. The collection of counter samples is performed over the largest temperature variation possible.

According to Procedure 1, the values of δC_1 , δC_2 , and δC_{12} are computed.

Procedure 1 Calibration:On_Fs_Interrupt

```

C1 ← Counter1.value
C2 ← Counter2.value
Counter1.reset()
Counter2.reset()
dC1 ← [C1 / (F0/Fs)] - 1
dC2 ← [C2 / (F0/Fs)] - 1
dC12 ← dC1 - dC2
print dC1, dC2, dC12

```

At the end of the calibration phase, the system has collected a set of $\langle \delta C_{12}, \delta C_1 \rangle$ and $\langle \delta C_{12}, \delta C_2 \rangle$ tuples. It is found that these tuples fit well to a third order polynomial function such that only the values of A , B , C , and D in the following equation are required to be stored:

$$\delta C_1 = A \cdot (\delta C_{12})^3 + B \cdot (\delta C_{12})^2 + C \cdot \delta C_{12} + D \quad (3)$$

3.2 Compensation Phase

The compensation phase performs a continuous frequency correction at run time to provide a higher stability clock. Instead of stabilizing f_1 or f_2 , using hardware based tuning circuits, we focus on regenerating a replica of the stable sampling clock, F_s from the unstable clock sources. The key idea of the compensation algorithm is to estimate the frequency of the sampling clock as closely as possible.

Procedure 2 Compensation:Initialization

```

gamma ← F0/Fs
RealTime ← 0
Timer1.value ← gamma
Timer1.reset()
Counter1.reset()
Counter2.reset()

```

As shown in the initialization routine in Procedure 2, the timer is loaded with a value $\gamma = F_0/F_s$ since this provides the best initial estimate of the sampling signal. On every timer interrupt, a sampling and compensation routine is executed as shown in Procedure 3.

Procedure 3 Compensation:On_Timer_Interrupt

```
//Read and reset counters
C1' ← Counter1.value
Counter1.reset()
C2' ← Counter2.value
Counter2.reset()
// Calculate the normalized difference
dC12' ← (gamma - C2') / (F0/Fs)
//Calculate the correction term
dC1' ← A · (dC12')3 + B · (dC12')2 + C · dC12' + D
gamma ← (F0/Fs) · (1+dC1')
//Increment the corrected counter
RealTime ← RealTime + 1/Fs
//Update the timer
Timer1.value ← gamma
```

Using the values of A , B , C and D from the calibration phase, $\delta C'_1$ is computed as:

$$\delta C'_1 = A \cdot (\delta C'_{12})^3 + B \cdot (\delta C'_{12})^2 + C \cdot \delta C'_{12} + D \quad (4)$$

$\delta C'_1$ represents an estimate of the mean relative drift of f_1 with respect to F_0 over the sampling period. Compensating for this drift would require to retune the oscillator such that f_1 is reduced by an amount $-F_0 \cdot \delta C'_1$. Instead, we compensate by continuously adjusting the value of γ such that $f_\gamma \approx F_s$ as follows:

$$\gamma = (1 + \delta C'_1) \frac{F_0}{F_s} \quad (5)$$

γ is then loaded into the timer for the next sampling period. By adjusting the value of γ in this way, we create as close a replica of the reference sampling signal as possible, accumulating *real time* epochs in the *RealTime* register as described below.

3.3 Corrected Timestamping

In order to use the above technique to estimate real time, a memory register *RealTime* is used to keep track of the accumulated counts. At every sampling interrupt, this register is incremented by a fixed value $1/F_s$ as shown in Procedure 4.

Procedure 4 Compensation:On_Get_Time

```
// Return RealTime's value and add the corrected
// elapsed time since the last increment
Correction = Counter1.value · (1/Fs) · (1/gamma)
return RealTime + Correction
```

4. EVALUATION

In order to prove the utility of our system, we must answer a series of questions: (1) Do the crystals really deviate with temperature? (2) Do different crystals deviate with temperature with different slope (stronger or weaker dependence with respect to another crystal)? (3) Can we measure

this difference with sufficient resolution? (4) Does this difference result in a significant improvement in accuracy over the longer term (sufficient to justify the existence of an XCXO)? and, finally, (5) can an XCXO actually be implemented in a low-cost microprocessor? We endeavoured to answer these questions by dividing the design and analysis process into three phases.

4.1 Feasibility Study

Answering the first question proved remarkably simple. Manufacturer-supplied data as well as our own lab measurements confirmed quite readily and very early on that the crystals vary significantly with temperature. Consequently, in this phase, the majority of our efforts were focused in examining the exact nature of this dependence and the impact of cut angle on the quartz crystal resonance. We implemented a CMOS-inverter based Colpitts oscillator design (similar to the one used in most modern microprocessors) and a motional arm model of the quartz crystal in Cadence Capture XL with pSpice A/D (part of the PSD 15.7 suite) to study the effects of loading and different cut angles based on measured data provided by Fox Electronics, a crystal manufacturer. Figure 2 depicts the frequency drift for different AT-cut crystals. To explore issues pertaining to quantization error and minimum required difference measurement resolution the entire XCXO algorithm was built in Matlab R2007A.

4.2 Environment Emulator

Having obtained sufficient confidence in the design fundamentals, we proceeded to the next evaluation phase where we explored the long term performance of the architecture. To do this we created an emulation platform that consisted of two Agilent 33220A arbitrary waveform generators. Each was programmed with the temperature-frequency curve of a differently cut crystal (we used 35°21' and 35°28') and could therefore, when taken together, reproduce the oscillatory behavior of our XCXO design proposal under any arbitrary temperature condition without the need for a thermal chamber and without the delay inherent in actually altering ambient conditions.

Using this platform to emulate the XCXO's hardware under environmental conditions and implementing the XCXO's software on a TI MSP430F1611 microprocessor, we were able to validate our phase I findings from Matlab using real hardware.

We want to show the impact on time keeping for a real-life scenario and compare our XCXO to a commercially available TCXO [14] and the uncompensated clock. We use temperature data collected by the Mossam project [15] while deployed in the James Wildlife Reserve from October 1st, 2004 to November 10th, 2007. The top plot in Figure 5 shows the temperature over the full time span. The temperature ranges from -12°C to 34°C, and one can clearly see the daily variations, as well as the seasonal changes in mean temperature. We employed these sensor traces in our emulator to stress an uncompensated AT-cut crystal, our XCXO compensated clock, as well as a TCXO (subplots 2, 3, and 4 in Figure 5).

Using these numbers, we can calculate the accumulated time error over time. The uncompensated clock performs the worst and accumulates a time shift of 960.8 seconds over the 3 year period. The TCXO performs much better and accu-

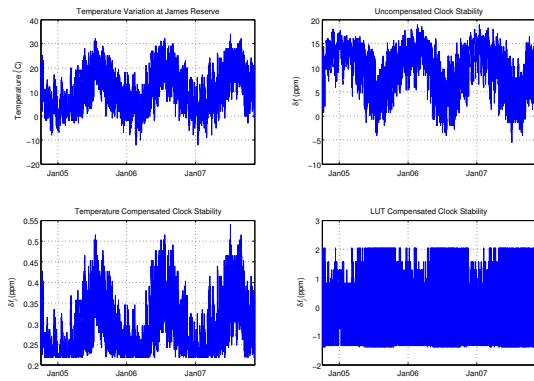


Figure 5: Clock stability using a real-life temperature data set. One can clearly see the daily temperature swings, as well as the seasonal changes in temperature, and how it affects the different compensation schemes.

mulates only 30.1 seconds, and the best is the XCXO which accumulates only a 3.3 second time shift over the whole 3 years. These numbers correspond to a mean effective stability over the full 3 year period of 10.13ppm for the uncompensated, 0.32ppm for the TCXO, and only 0.04ppm for the XCXO respectively. This shows that there is a tremendous potential for timekeeping by employing more accurate clocks, and our XCXO compensated clock even outperforms a commercially available TCXO by a factor of 8 over temperature ranges occurring in a real deployment. Furthermore, the XCXO compensated clock doesn't require costly and power hungry TCXO hardware.

4.3 XCXO Implementation

In the final phase of our work, We implemented the XCXO as a small hardware module which we integrated into a readily available platform widely used in Sensor Network research – the Moteiv TMote Sky [11]. The TMote Sky is based on the TI MSP430F1611, which we had previously employed and it offered both low-power operation and a set of requisite peripherals desirable to our approach.

4.3.1 Hardware Considerations

To achieve the integration of the XCXO, we modified the TMote by removing its standard 32kHz crystal and replacing it with our XCXO. We fabricated the XCXO in 1oz. copper clad double-sided FR-4, which we milled on our in-house LPKF C40 Promomat CNC mill. The toolchain used to achieve this included Cadence OrCAD Layout Plus 15.7 (layout), Gerbtool 14.2 (post-processing), CircuitCAM 4.0 (fabrication setup), and BoardMaster 4.0 (milling control). Figure 6 shows a picture of the hardware modification.

As our environmental emulator revealed, very small manufacturing differences in the crystal (in the case of our emulator, just 7 arcmin!) can generate a measurable differential drift of sufficient magnitude to allow compensation to our targeted accuracy levels. Consequently, we chose two crystals from two different manufacturers in order to achieve this difference in the temperature behavior. As shown in Section 4.3.3 this logic proved correct. The two crystals in our prototype are (1) Kyocera HC49SFWB [12] and (2) FOX HC49SDLF [13]. Both crystals operate at their fundamental resonance frequency (nominally 8.000 MHz) and have a ± 50 ppm accuracy over the commercial temperature range.

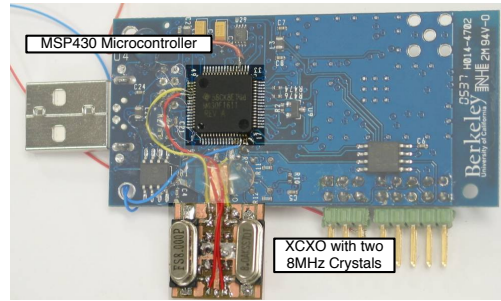


Figure 6: The modifications to the TMote Sky platform are minimal. We added a small circuit board that contains the two 8MHz crystal oscillators.

4.3.2 Software Considerations

Interrupts on microprocessors have the tendency to be serviced with non constant latency. For that reason, we have to make sure that interrupt latency and interrupt jitter don't affect our measurements in our hardware implementation. Therefore, we make extensive use of the MSP430's Timer features. Two key features are the timer capture and the timer output. The timer capture allows us to trigger the reading of the timer value by an external signal on an input pin. When the input pin transitions from low to high, the value of the timer is stored in a temporary register and an interrupt is sent to the microprocessor. The application can then read that register and gets an accurate reading of when the signal transitioned, regardless of how much latency the microprocessor takes to service the interrupt.

Similar to the timer capture, the timer output allows an application to toggle an output pin at a specific time of the timer. The application writes the time it wants the pin to be toggled into a predefined register. When the timer reaches that value, it will automatically toggle the output pin and send an interrupt back to the application. Both techniques, timer capture, and timer output, are necessary to achieve a high accuracy in the calibration, as well as compensation phase.

4.3.3 Platform Testing

We tested the hardware implementation by subjecting the platform to a temperature variation from 23° to 36°C while running the calibration algorithm. The temperature chamber was a simple Styrofoam box with a heating element. The temperature sensor was a Go!Temp USB probe. The reference clock is a simple timing unit hold at constant temperature. The timing unit generates a 1Hz signal which we feed into our Microprocessor's timer capture units. Figure 7 shows the preliminary result for this small temperature variation after applying the calibration algorithm. We can already see that the two used crystals behave slightly different under the same temperature environment. This is exactly what we are looking for and are exploiting in our compensation algorithm. Figure 8 illustrates this even better. We can see that the crystals have a different slope even over the small temperature variation of 13°C.

In Figure 7 we can see that the crystals don't return on the exact same path if you heat them, or if you cool them down. This is an artifact of how we measure the temperature inside our test equipment. Our temperature probe measures the ambient temperature, not the actual temperature of the crystal itself. Thus, we observe a small offset between what

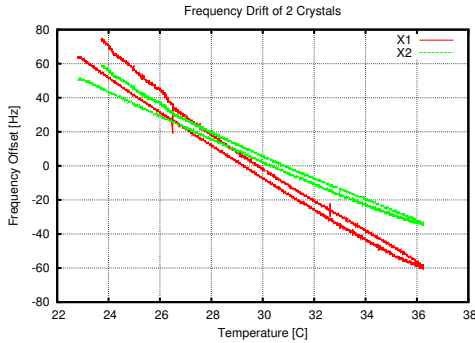


Figure 7: Frequency offset from the nominal 8MHz for the two crystals. Note the different slope which we exploit in our algorithm.

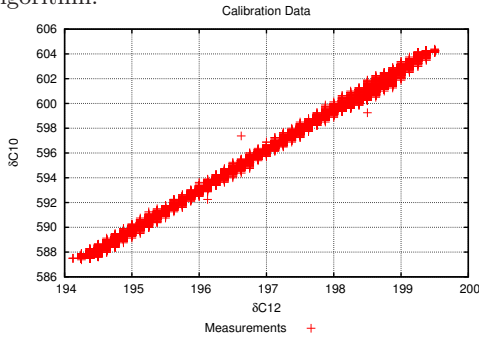


Figure 8: Calibration measurements of the two 8MHz crystals over a temperature range of 13°C. the crystals experience and what we measure.

5. CONCLUSION

Building Wireless Sensor Networks for long-term environmental monitoring and safety applications is a demanding task constrained on both sides of the price-performance curve by large quantities forcing reduced costs and long lifespans forcing minimal power (maximal clock performance). To return to our initial discussion of performance targets introduced in Section 1, again consider that communicating nodes with clock drifts of $\pm 50\text{ppm}$ force the lower bound on duty cycling up to 0.01% [16]. Using the formula, $DC = 2 * \delta f + \frac{t_{pkt}}{T_{pkt}}$, taken from [16], where t_{pkt} is the time it takes to send a packet, and T_{pkt} the packet interval, we can calculate that our XCXO compensated clock pushes the lower bound of the duty cycle to $8 \cdot 10^{-6}\%$. In practice, this rate is unattainable as radio speed and radio wakeup (impacts t_{pkt}) and the rate at which packets are sent now clearly dominate the possible duty cycle. In effect, we have provided accuracy sufficient to completely remove the clock source as the bottleneck in network lifetime at a fiscal cost well below the cost of the next-best technology employed in practice today (TCXO or OCXO).

To proffer a sense of scale, our XCXO design can provide near 1 sec per year drift independent of temperature and in an energy budget low enough and a package small enough to meet the complex challenges of outdoor wireless sensor network deployments and at the time of this writing is the only system in publication to be able to do so.

Our work, thus far, in the exploitation of this differential quartz resonator effect is just the beginning of what this technology can offer. We are currently exploring "difference

amplifiers" in the oscillator circuit. By combining the cubic dependence of the quartz crystal with the quadratic dependence of a Y5V rated capacitor installed to load each of the XCXO's crystals independently (and choosing crystals with wide pole-zero spacing), we may be able to produce even sharper differential traits, which would allow even higher accuracy from the same nominal-frequency parts we are using now – or allow our current accuracy levels from even lower nominal-frequency valued crystals, shaving even more power from the WSN energy requirements with a corresponding increase in network runtime. We are also working on migrating the design to an ip core suitable for integration as a peripheral unit in a microprocessor or as a functional unit in an ASIC.

6. REFERENCES

- [1] *MIL-O-55310, Military Specification for Oscillators, and Crystal*, Military Spec. and Standards, 2007.
- [2] IEEE Standards Board, "IEEE guide for measurement of environmental sensitivities of standard frequency generators," *IEEE Std 1193-1994*, 27 Feb 1995.
- [3] D. Newell and R. Bangert, "Temperature compensation of quartz crystal oscillators," *17th Annual Symposium on FCS.*, pp. 491–507, 1963.
- [4] D. Newell and H. Hinnah, "Automatic compensation equipment for tcxo's," *22nd Annual Symposium on FCS. 1968*, pp. 298–310, 1968.
- [5] W. Zhou, H. Zhou, Z. Xuan, and W. Zhang, "Comparison among precision temperature compensated crystal oscillators," *Frequency Control Symposium and Exposition, 2005.*, 29-31 Aug. 2005.
- [6] K.-S. Shin and W.-Y. Chung, "Automatic tcxo frequency-temperature test chamber using thermoelectric device array [temperature compensated crystal oscillator]," *ISIE*, vol. 3, pp. 1624–1627, 2001.
- [7] K. Kubo and S. Shibuya, "Analog tcxo using one chip lsi for mobile communication," *FCS Symposium, 1996.*, pp. 728–734, 5-7 Jun 1996.
- [8] V. Candelier, G. Caret, and A. Debaisieux, "Low profile high stability digital tcxo: ultra low power consumption tcxo," *FCS, 1989.*, 31 May-2 Jun 1989.
- [9] S.-J. Lee, J.-H. Han, S.-H. Hank, J.-H. Lee, J.-S. Kim, M.-K. Je, and H.-J. Yoo, "One chip-low power digital-tcxo with sub-ppm accuracy," *ISCAS 2000*, vol. 3, pp. 17–20 vol.3, 2000.
- [10] M. Li, X. Huang, F. Tan, Y. Fan, and X. Liang, "A novel microcomputer temperature-compensating method for an overtone crystal oscillator," *IEEE Transactions on UFFC*, vol. 52, no. 11, Nov. 2005.
- [11] Moteiv, "TMote Sky Datasheet."
- [12] "Kyocera HC49SFWB Datasheet," http://global.kyocera.com/prdct/electro/pdf/xtal/102_e.pdf, 2007.
- [13] "Fox HC49SDLF Datasheet," www.foxonline.com/pdfs/hc49sdlf.pdf, 2007.
- [14] "DS4026-10MHz to 51.84MHz TCXO," *Maxim Integrated Products, Dallas Semiconductor*.
- [15] James Reserve, "MossCam," <http://www.jamesreserve.edu/mossCam/>, 2007.
- [16] P. Dutta, D. Culler, and S. Shenker, "Procrastination might lead to a longer and more useful life," *HotNets-VI*, 2007.